Global and Planetary Change 75 (2011) 56–66

Contents lists available at ScienceDirect

Global and Planetary Change

journal homepage: www.elsevier.com/locate/gloplacha

Palynological evidence for Neogene environmental change in the foreland basin of the southern Tianshan range, northwestern China

Zhenqing Zhang, Jimin Sun *

Key Laboratory of Cenozoic Geology and Environment, Institute of Geology and Geophysics, Chinese Academy of Sciences, P. O. Box 9825, Beijing 100029, China

ARTICLE INFO

Article history:
Received 5 September 2010
Accepted 15 October 2010
Available online 23 October 2010

Keywords:
Tianshan range
Tarim Basin
neogene
pollen
paleoclimate

ABSTRACT

In this paper, we report 3780-m-thick Neogene deposits accumulated in the Kuqa foreland basin of southern Tianshan range, providing great potential for studying both tectonics and paleoclimatic changes. Based on palynological evidence, we discuss the paleoenvironmental changes as well as the interplay between regional uplift and climatic change in the region studied. Our results indicate that the vegetation and climatic changes from 13.3 to 7 Ma were response to global climatic changes. After 7 Ma, the uplift of the southern Tianshan range partially affects vegetation and climatic changes. Both global cooling and the rainshadow effect of uplifted high mountains affect the enhanced arid climate initiated ca. 5.23 Ma ago. Such climatic changes are important archives in reconstructing paleoclimate of the Asian interior.

1. Introduction

The Asian interior consists of several Asia's major mountain ranges, forming a series of mountain–basin systems. These mountains are characterized by vertical biological diversity, whereas dry climate prevails in lower lands and basins forming vast deserts (e.g., Kara Kum, Kyzyl Kum, Taklamakan, and Junggar). It is an interesting question as to study the paleoenvironment and arid history in the Asian interior.

Among the large inland basins in central Asia, the Tarim Basin is the most famous for its large area (~560,000 km^2) and active sand dunes. This basin is constrained by three largest Asia's mountain ranges, the Tianshan range to the north, the Pamir Mountain to the west, and the Kunlun range to the south (Fig. 1a). The climate is extremely dry, and annual rainfall is mostly less than 50 mm. It is the driest region in the Asian interior. The late Cenozoic was a time of major climate and vegetation changes. Compared with the extensive pollen records from the other sites of China (e.g., Wang, 1990; Hu and Sarjeant, 1992; Liu and Leopold, 1994; Ma et al., 1998, 2004; Liang et al., 2003; Sun and Wang, 2005; Sun et al., 2007; Sun and Zhang, 2008; Xu et al., 2008), less is known about the long-term vegetation changes in the Tarim Basin. The objective of the present work is to use pollen data to reconstruct vegetation changes in the inland basin of the Asian interior.

2. Geological setting, geography and vegetation

The studied region is the foreland basin of the southern Tianshan range (Fig. 1a). Thick Cenozoic deposits accumulated in the foreland basin, forming a series of elongated anticlines, paralleling to the Tianshan orogenic belt, indicating a Cenozoic north–south contraction and crustal shortening (Fig. 1b). Such thrusting and folding systems are evidence of the reactivation of the Paleozoic orogenic belt (e.g., Allen et al., 1992; Gao et al., 1998) during the Cenozoic era (e.g., Avouac et al., 1993; Hendrix et al., 1994; Yin et al., 1998; Burchfiel et al., 1999; Deng et al., 2000; Fu et al. 2003, 2010; Charreau et al., 2006; Huang et al., 2006; Sobel et al., 2006; Hubert-Ferrari et al., 2007; Sun et al., 2004, 2009; Sun and Zhang, 2009). These anticlines are associated with the deep thrust faults as a consequence of southward thrusting of the southern Tianshan (e.g., Tang et al., 2004; Jin et al., 2008). The Klasu structural belt (Fig. 1b), to the north most, consists of several shallow anticlines. The second thrusting and folding belt is the Qiulitag Anticline, which is a west–east stretching mountainous ridge that extends 340 km with a 5–7 km width (Fig. 1b). The Qiulitag Anticline is a fault related fold (Hubert-Ferrari et al., 2007), both the age of the deposits and the tectonic structures change spatially. The Yaken Anticline, to the south most, is characterized by the gentle topographic relief, stretching about 80 km with a width of 8–10 km (Fig. 1b).

Our study focused on the Kuchetawu section (41°55.097′N, 83°03.280′E), it is part of the Qiulitag Anticline, exposed (transection A–B, Fig. 1b) by the southward flowing Kuqa River. Field investigations indicate that it is an overturned fold, consisting of steep strata in the core and gentle dip strata in the limbs (Fig. 2). This anticline exposes the middle Miocene Jidike Formation in the core, and the late

* Corresponding author. Tel.: +86 10 8299 8389; fax: +86 10 6201 0846.
E-mail address: jmsun@mail.igcas.ac.cn (J. Sun).

0921-8181/$ – see front matter © 2010 Elsevier B.V. All rights reserved.
doi:10.1016/j.gloplacha.2010.10.006

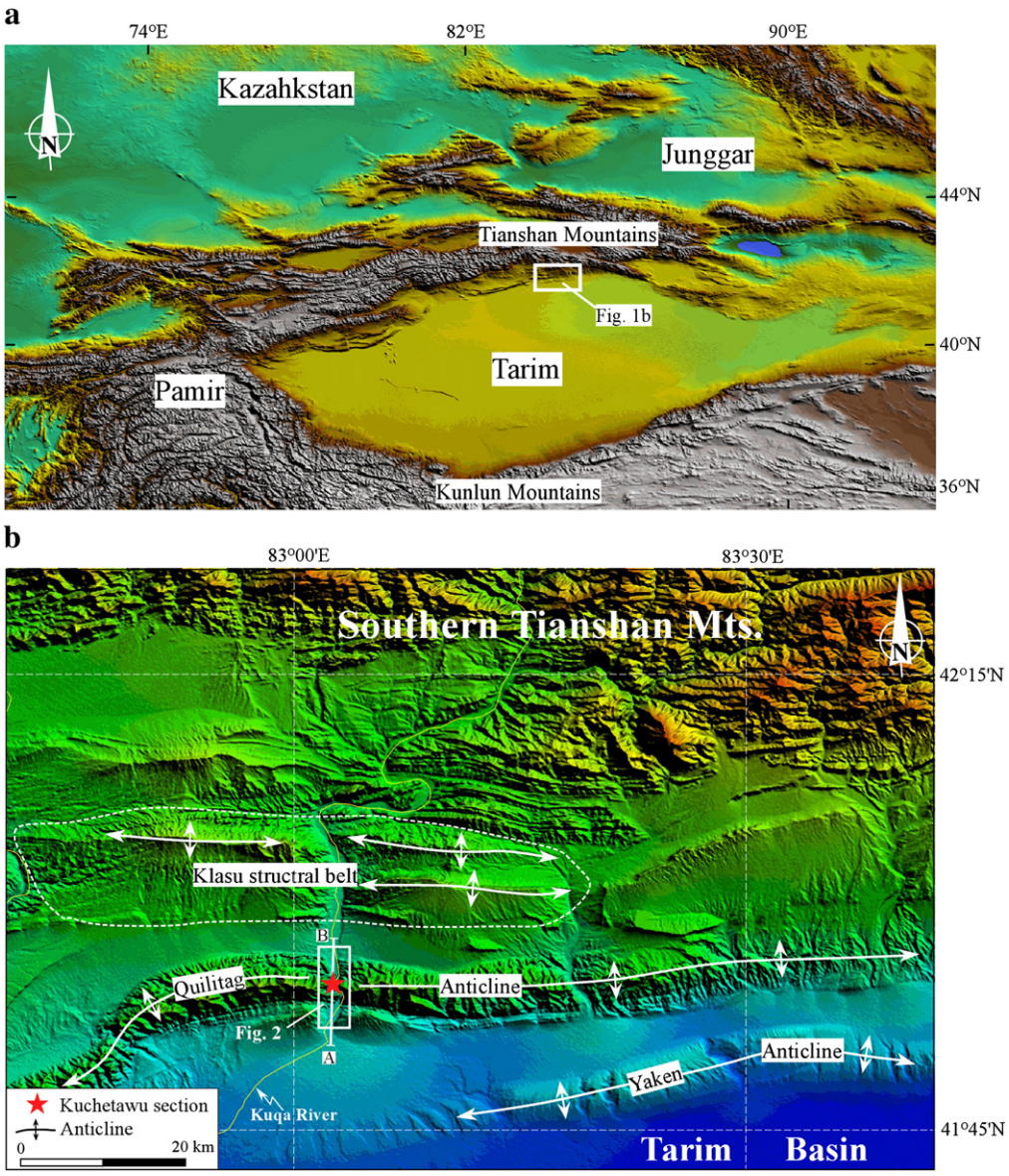

Fig. 1. Digital elevation model image of the Tarim Basin and surrounding region (a) and topographic map of the study area (b, modified from Sun et al., 2009).

Miocene Kangcun Formation, Pliocene Kuqa Formation and the Lower Pleistocene Xiyu Formation in the southern flank (Fig. 2). Compared with the southern limb, there is only relict Kangcun Formation in its northern limb. Therefore, our sampling began from the core to its southern limb (Fig. 2).

Generally, there is a trend of towards coarser particle size and more gravels in this section. The oldest stratum is the Jidike Formation (N_{1j}), it is dominated by reddish mudstones with occasionally grey sandstone or siltstone intercalations (Fig. 3a), and its thickness is 1170 m. The Kangcun Formation (N_{1k}) consists of interbedded grey sandstones and reddish to brownish mudstones (Fig. 3b), and its thickness is 1770 m. The Kuqa Formation (N_{2k}) can be subdivided into two parts: the lower part is composed of interbedded grey conglomerates and brownish mudstone or siltstone; while the upper part is

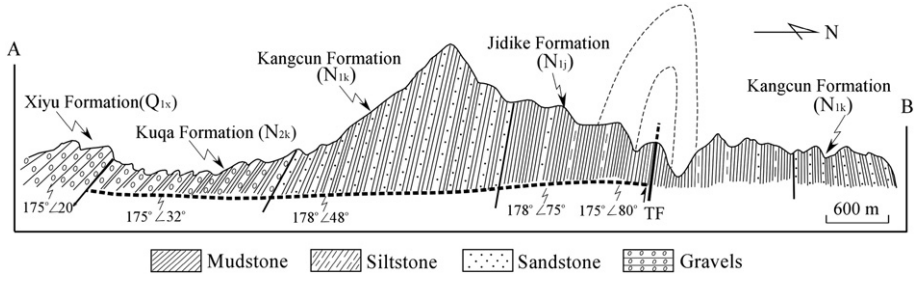

Fig. 2. The exposed Cenozoic strata of the Kuchetawu section along cross-section A–B (from Sun et al., 2009, see Fig. 1b for location), cut by the Kuqa River. The bold dashed line in the lower part shows the sampling route. N_{1j}: Middle Miocene Jidike Formation; N_{1k}: Late Miocene Kangcun Formation; N_{2k}: Pliocene Kuqa Formation; Q_{1x}: Early Pleistocene Xiyu Formation; and TF: Thrust Fault.

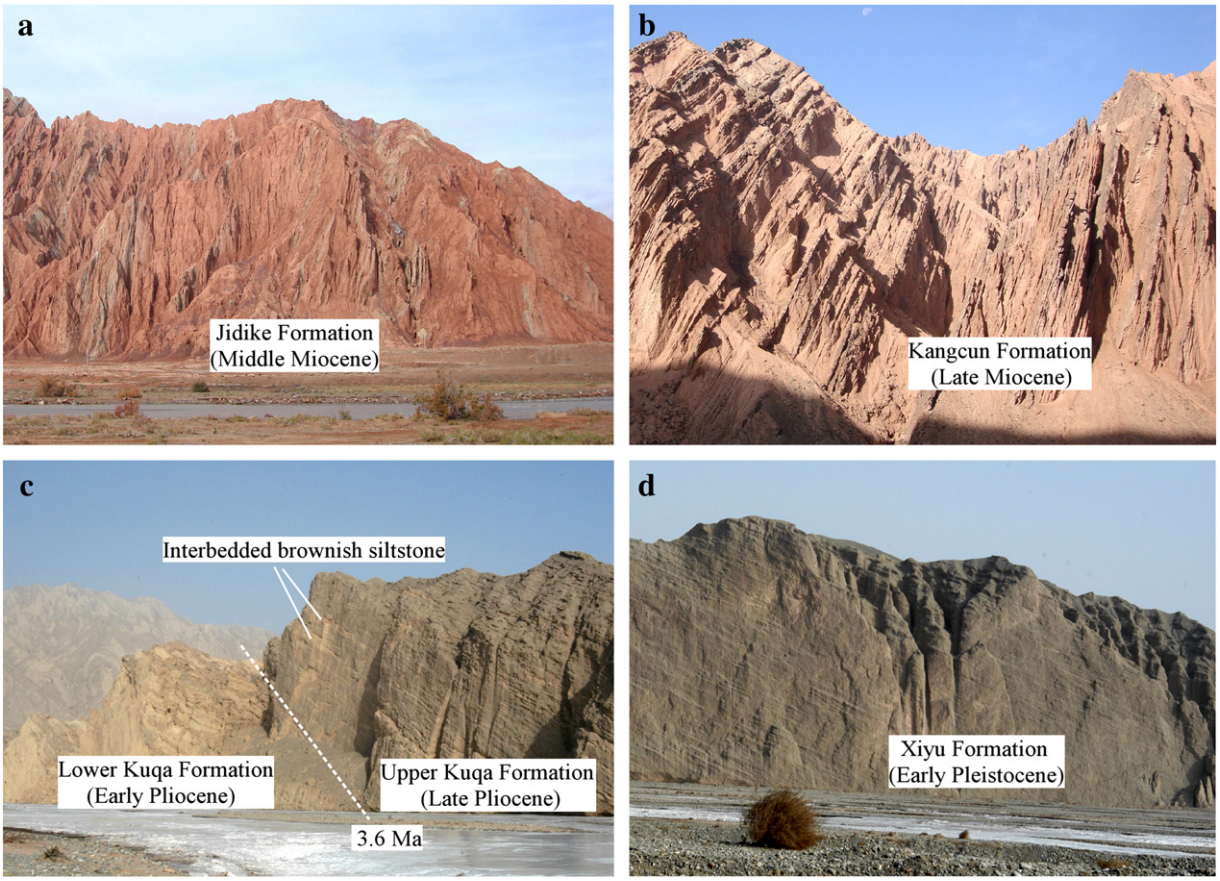

Fig. 3. Photos show the folded Cenozoic strata along the southern limb of the Kuchetawu anticline. (a) Dominated reddish mudstone of the Jidike Formation; (b) interbedded of grey sandstones and reddish to brownish mudstones of the Kangcun Formation; (c) interbedded grey conglomerates and brownish mudstone or siltstone of the Kuqa Formation; and (d) massive grey conglomerates of the early Pleistocene Xiyu Formation.

dominated by grey conglomerates with thin intercalated brownish siltstone layers (Fig. 3c). The thickness of the Kuqa Formation is 840 m. The Xiyu Formation (Q_{1x}) is a marker bed for regional stratigraphic correlation; it consists of massive conglomerates (Fig. 3d), thus impossible for our pollen sampling, and its thickness exceeds 1000 m.

The present precipitation and vegetation vary with elevations of the southern Tianshan range. The annual precipitation ranges from less than 100 mm at lower elevations to 250–450 mm at elevations of higher than 2000 m in its southern slope. In the study region, the present-day mean annual temperature is 11.4 °C, and the mean annual precipitation is 64.5 mm. The vertical changes of the climate maintain diverse vegetation on the south-facing slope of the southern Tianshan range (Fig. 4). Alpine meadows occur at elevations of 2800–3500 m above sea level (asl) dominated by *Kobresia myosuroides, Carex polyphylla*, *Kobresia humilis,* and *Juncus triglumis*. Alpine steppe dominated by *Stipa spp., Poatibetica, Androsace sericea, Seriphidium transiliensis, Oxytropis rupifraga*, and *Potentilla asiaemediae* occurs at

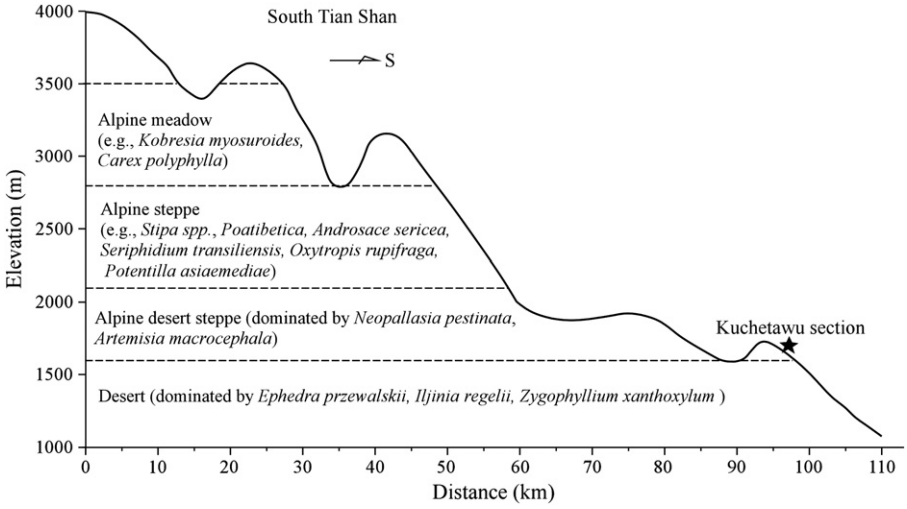

Fig. 4. Present-day vertical distribution of vegetation belts upon the southern slopes of the Tianshan range.

2100–2800 m asl. Alpine desert steppe dominated by *Neopallasia pestinata,* and *Artemisia macrocephala* occurs at elevations of 1600–2100 m asl, and desert dominated by *Ephedra przewalskii, Iljinia regelii,* and *Zygophyllium xanthoxylum* occurs below 1600 m asl.

3. Materials and methods

We collected 185 samples from the 3780 m thick sediments for palynological analysis. At least 100 g of sediment was used for each sample in order to acquire enough pollen grains. Samples were treated with HCl (35%) and HF (70%) to remove carbonates and silica. Separation of the palynomorphs from the residue was performed by using $ZnCl_2$ (density = 2), following the method of Faegri and Iversen (1989). Slides were prepared by mounting the pollen grains in glycerin jelly, and then counted under a microscope using ×400 magnifications. Pollen identifications were performed using the pollen flora of China (Wang et al., 1997). For each sample, pollen grains were counted until a minimum pollen sum of 200 grains was reached.

We also performed a principal component analysis (PCA) for the pollen data, which transforms a number of possibly correlated variables into a smaller number of principal components. The results of a PCA are usually discussed in terms of component scores and loadings (Shaw, 2003). In this study, pollen taxa reaching 5% or greater were included in the PCA analysis by using the statistic program CANOCO (ter Braak and Smilauer, 2002).

4. Results

4.1. Chronology

The chronology of the Kuchetawu section is based on both biostratigraphic age control and high resolution magnetostratigraphy. As we know, it is crucial to have biostratigraphic age control for thick (commonly thousands of meters) Neogene deposits in foreland basins. During our field expedition, we discovered a tooth fossil of *Hipparion* at a depth of 3100 m (Fig. 5). Further laboratory works identified it to be *Hipparion chiai*. This kind of fossil belongs to the Bahe fauna in China (Li et al., 1984; Deng and Wang, 2004), corresponding to Vallesian Age of the European Neogene mammal zones (MN) 9/10 (Deng, 2006), with an age range of 11–9 Ma and centered at about 10 Ma. Moreover, the extremely thick (>1000 m) massive conglomerates of the Xiyu Formation is a marker stratum in the foreland basins of northwestern China, and its basal age has been proposed to be near the Pliocene/Pleistocene boundary (e.g., Huang et al., 1947; Peng, 1975).

Based on the above biostratigraphic age constraints, we compared the measured magnetic polarity sequence of the studied section with the geomagnetic polarity timescale (GPTS) of Cande and Kent (1995) (Sun et al., 2009), yielding an age range of 13.3 to 2.6 Ma for the studied section (Fig. 5).

The base of the uppermost Xiyu Formation is 2.6 Ma. The upper Kuqa Formation, dominated by conglomerates but with thin siltstone intercalations, has a basal age of 3.6 Ma, while the lower part of this formation corresponds to an age of 5.23 to 3.6 Ma. Therefore, the Kuqa Formation has a Pliocene age. The Kangcun Formation has an age of 9.7–5.23 Ma, while the Jidike Formation was accumulated between 13.3 and 9.7 Ma (Fig. 5). Therefore, our results indicate that: (1) the basal age of the studied section is 13.3 Ma, and the age range of the measured sequence is between 13.3 and 2.6 Ma; and (2) there is a remarkable lithological shift at 5.23 Ma, marked by change from dominant fine-grained fluvial-lacustrine deposits to fan-fluvial coarse deposits with commonly interbedded conglomerates (Fig. 5).

4.2. Pollen results

The pollen result is shown in a pollen percentage diagram (Fig. 5), and photographs of selected pollen grains are in Figs. 6 and 7.

The main characteristics of the pollen diagram show that: (1) the entire section is dominated by tree pollen, of which *Pinus* and *Betula* are the most abundant pollen elements, and the other tree taxa of *Abies*, *Quercus*, *Picea* and *Ulmus* are also common; and (2) among the herbs, *Artemisia* and Chenopodiaceae are the most common taxa (Fig. 5). Although most of the pollen taxa do not show remarkable variations, the pollen diagram can be generally zoned by visual inspection (Fig. 5).

The basal pollen zone I (PZ-I, 3780–1900 m depth, ca. 13.3–7 Ma) is characterized by the lowerst percentage of high-altitude conifer *Abies*. Additionally, among the thermophilic taxa, *Corylus* and *Carpinus* are the highest of the whole section, while the other pollen taxa including *Juglans* and *Quercus* only show slightly higher than the other pollen zones. The pollen spectra of PZ-I are dominated by *Betula*, *Pinus*, *Quercus*, and *Picea*.

PZ-II (1900–800 m depth, ca.7–5.23 Ma) is notable for the abrupt increase and very high percentage of boreal conifer *Abies* (Fig. 5). Moreover, the abundance of *Betul*a is the highest, whereas *Pinus* is the lowest of the section. Compared with PZ-I, the abundance of *Artemisia* shows a slight increase. The pollen spectra of PZ-I are dominated by *Betula*, *Pinus*, *Abies*, *Quercus*, and *Picea*.

PZ-III (800–0 m depth, ca. 5–2.6 Ma) is notable for the highest abundance of *Artemisia*. The percentage of *Picea* and *Juglans* is the lowest. The pollen spectra of PZ-III are dominated by *Pinus*, *Betula*, *Artemisia*, *Abies*, and *Quercus* (Fig. 5).

5. Discussions

Pollen records from the foreland basin of the southern Tianshan range can be influenced by lithofacies, climate change, and tectonic-induced changes in altitude. In order to convincingly reconstruct the past environment, we need to consider the above factors in interpretation of the pollen data.

5.1. Lithofacies and depositional environments

The Neogene strata in the study area are predominantly beds of mudstone, siltstone, sandstone and conglomerates with varied textures and lithofacies. We have identified three distinct lithofacies based on the lithology (Fig. 8). Generally, the sedimentary facies change from the basal lacustrine-fluvial deposition to upper fluvial-fan systems, accompanied by a general coarsening trend of the deposits. In the studied foreland basin, the pollen sources include fluvial transportation, wind transportation and *in situ* production. For the first case, the distance between the source materials and the depositional sites as well as the energy of the fluvial agency can influence the pollen concentration in the sediment. Therefore, in order to eliminate this influence, pollen palynological samples were obtained only from fine-grained horizons and no samples were from the coarse conglomerates. The vertical variations of the raw pollen counts versus depth are shown in Fig. 8, it clearly indicates that the curve is rather smooth compared with the changing lithology, suggesting that the pollen grains in the fine sediments are not significantly affected by lithofacies (Fig. 8).

5.2. Tectonic history in the studied foreland basin

It is important to have knowledge about uplift history in a tectonic active region in order to better interpret climatic implications of pollen record. In recent years, the exact timing of tectonics in this foreland basin has been an important issue (e.g., Charreau et al., 2006, 2008; Hubert-Ferrari et al., 2007; Huang et al., 2006, 2008; Sun et al., 2009). Huang et al. (2006) proposed two episodic uplifts occurring at 17–16 Ma and 7 Ma, respectively. Charreau et al. (2006) argued acceleration in the erosion and uplift of the southern Tianshan at 11 Ma. Hubert-Ferrari et al. (2007) suggested that crustal shortening initiated ~6 Ma. Sun et al. (2009) showed that evidence of uplift

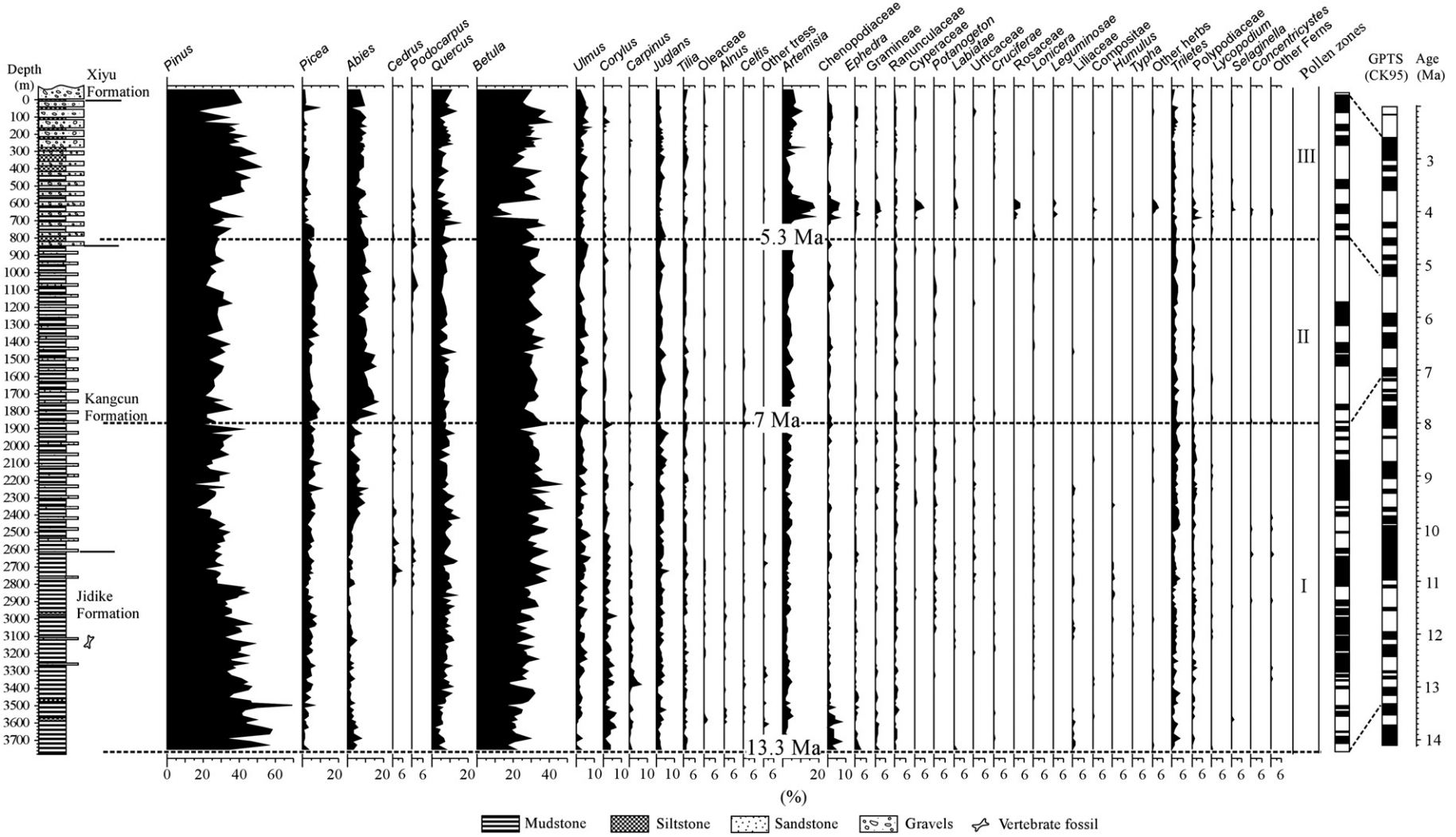

Fig. 5. Pollen diagram showing percentage abundances of pollen taxa within the Kuchetawu section. Age control is based on biostratigraphic constraints and measured magnetostratigraphy (Sun et al., 2009).

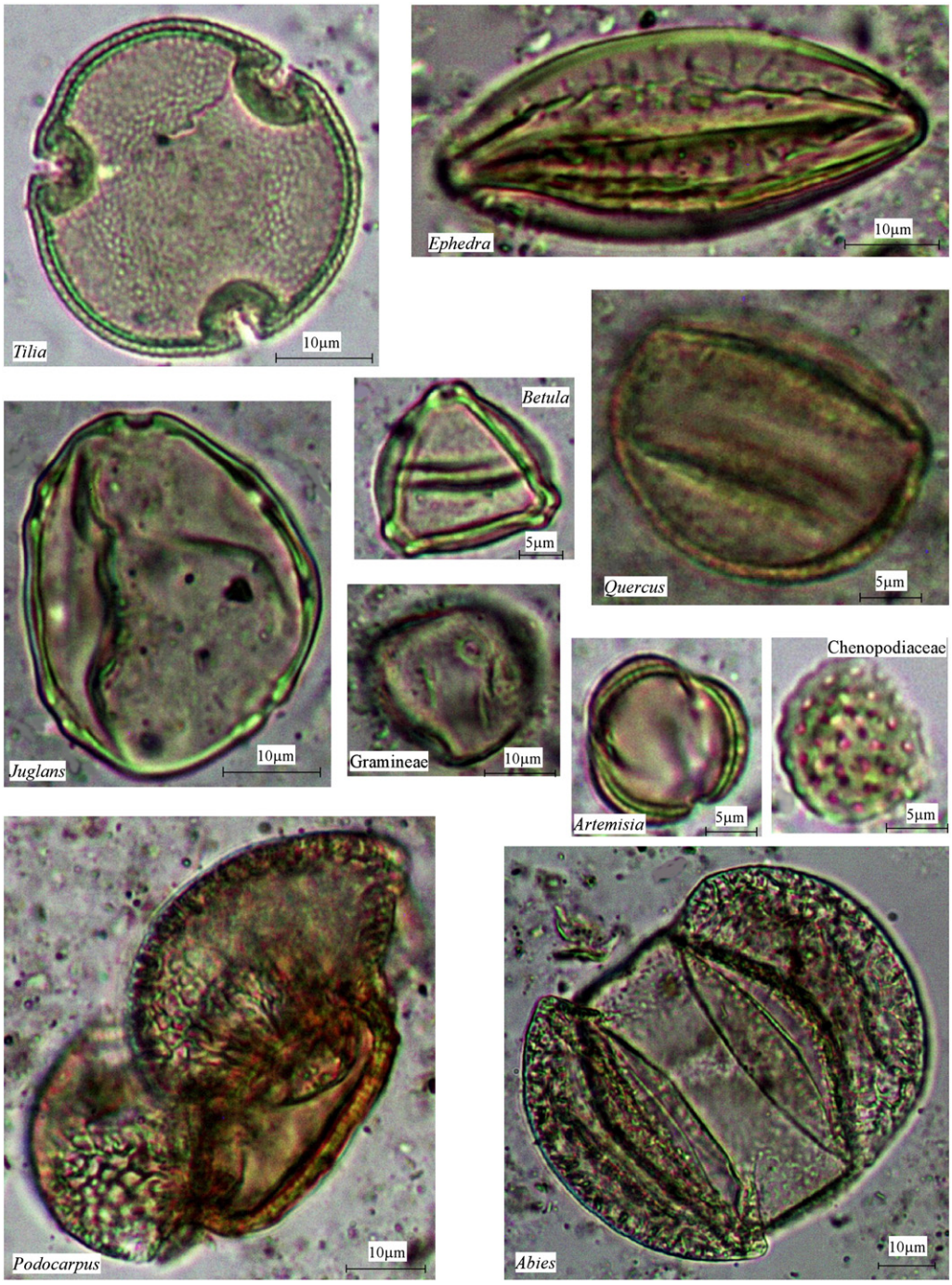

Fig. 6. Representative photographs of pollen grains from the Kuchetawu section.

initiated 7 Ma. Such differences in the mountain uplift of the same region are mostly due to the different methods used by authors. Both Charreau et al. (2006) and Huang et al. (2006) used rock magnetic characteristics and sedimentary rates to deduce the uplift history of the southern Tianshan range. As we know, the rock magnetic characteristics (anisotropy of magnetic susceptibility, AMS) are affected by many factors including sedimentary condensation, sedimentary facies, texture of sediments, source materials, and tectonic compression. In this sense, the AMS is not solely controlled by tectonics, therefore, care must be taken in using AMS to infer tectonic uplift. Moreover, in an active tectonic foreland basin, the accumulation rates of sediments are also controlled by multiple factors, including possible sedimentary hiatus, fluvial channel diversion, climatic change induced rock denudation, and tectonic uplift induced rock erosion. Thus, similar to the AMS, the sedimentary rates can be only used, to some extent, as an indirect parameter for mountain uplift. Different from the indirect evidence of AMS and sedimentary rates, Hubert-Ferrari et al. (2007) and Sun et al. (2009) explored the timing of syntectonic strata (growth strata) and proposed an acceleration of crustal shortening initiated ~6 and 7 Ma, respectively. The only difference is that Hubert-Ferrari et al. (2007) have not their own magnetostratigraphy but referenced the chronology of Charreau et al. (2006), while Sun et al. (2009) used their own chronology for getting the age of crustal shortening.

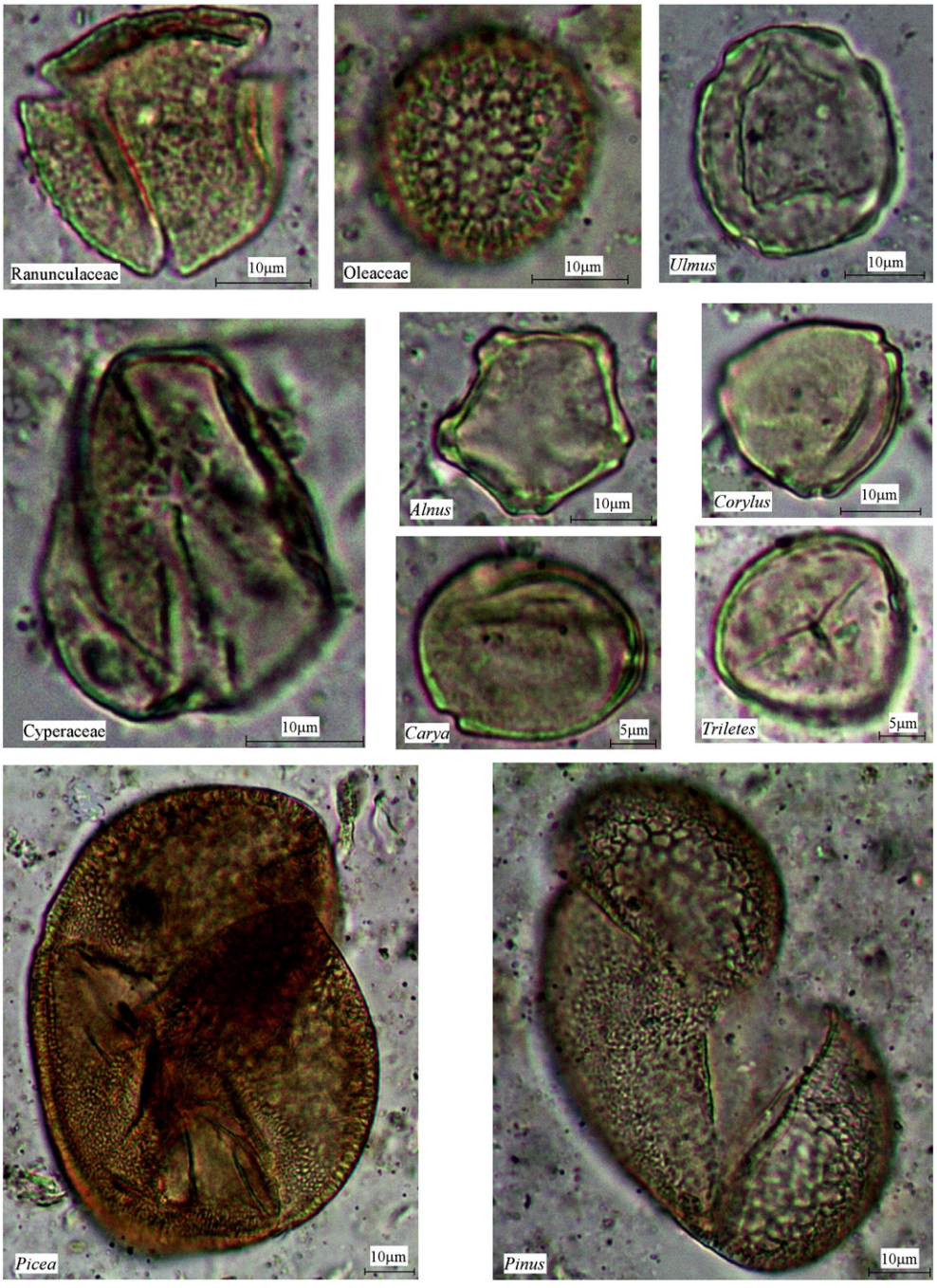

Fig. 7. Representative photographs of pollen grains from the Kuchetawu section (continued).

Our earlier evidence of crustal shortening and uplift event initiated ca. 7 Ma ago and lasted to the early Pleistocene (Sun et al., 2009), whereas the period of 13.3 to 7 Ma is characterized by dominant low-energy fine deposits and thus relatively stable tectonics.

Therefore, we only need to discuss the climatic effect on pollen record during the period of 13.3 and 7 Ma, but we must consider both the effects of tectonic uplift and climatic changes on the pollen assemblages after 7 Ma ago.

5.3. Relatively warm and humid climate between 13.3 and 7 Ma

During this period, the vegetation is characterized by the most abundant of temperate broadleaf deciduous pollen taxa of *Corylus* and *Carpinus,* and additionally the other thermophilic taxa of *Juglans* and *Quercus* also show slightly higher than the other period (Fig. 5). The cool-temperate or boreal taxon *Abies* is the minium of the whole section. Therefore, the characteristics of the PZ-I suggest a relative warm and humid climate compared with that of the other pollen zones.

In order to further investigate regional paleoenvironment, we use the PCA analyzing results to display past climatic changes. Fig. 9 shows a PCA biplot of the pollen percentages. The first principal component, axis 1, accounts for 30.4% of the variance in the pollen spectra; axis 2 accounts for 26.7%. The temperate deciduous *Corylus* pollen has the highest positive loadings (0.78) on axis 1, whereas the cool-temperate conifer *Abies* has the highest negative loadings (−0.87). Compared with the negative loadings of *Abies*, the positive loadings of *Corylus* on axis 1 suggest a warmer and more humid climate.

We also use the first and second axes of the PCA as a proxy for biotic variability through time (Fig. 10). The factor scores on axis 1

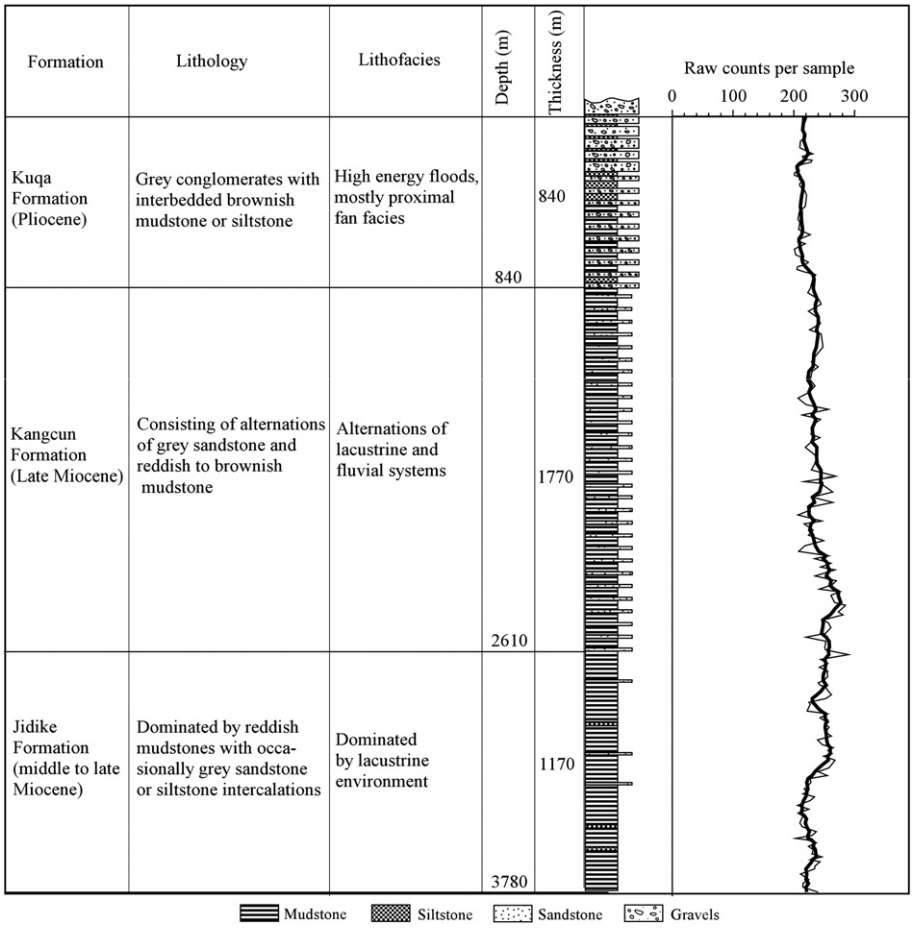

Fig. 8. Lithology, biostratigraphy, and vertical variations in raw pollen counts. The thick black line in the count data is a 5-point running average.

clearly show highest values at depths of 3780–1900 m, ca. 13.3–7 Ma. As the positive factor scores on axis 1 suggest a warmer and more humid climate, they indicate a relatively optimum climate compared with other periods. This is consistence with our interpretations based on pollen species.

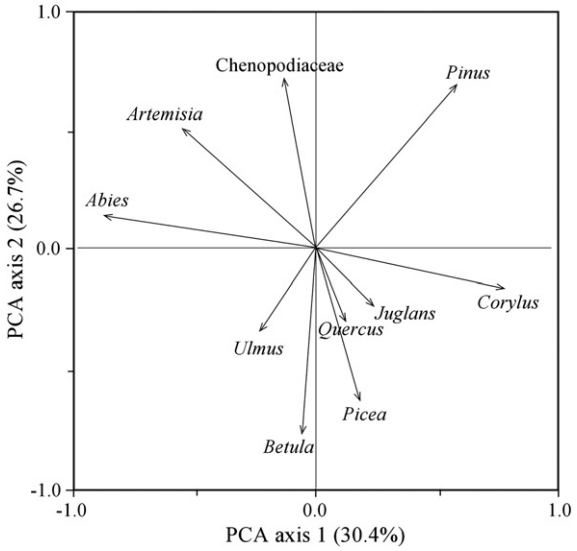

Fig. 9. Principal component analysis (PCA) biplot of pollen species from the Kuchetawu section. Axes 1 and 2 account for 30.4% and 26.7% of the variance in species abundances, respectively.

5.4. Increased high-altitude conifer Abies after 7 Ma and enhanced aridity since 5.23 Ma ago

The most remarkable feature of pollen spectra after 7 Ma ago is the abrupt increase of the high-altitude conifer *Abies*. The percentages of *Abies* can be influenced by both mountain uplift and climatic change. It is necessary to stress that our previous evidence demonstrated that a main phase of the regional uplift of the southern Tianshan range initiated ca. 7 Ma (Sun et al., 2009), the increased elevation would be favorable for the expansion of high-altitude pollen of *Abies*.

Additionally, the pollen spectra can be also influenced by climatic changes. Fig. 5 shows that the percentages of warm-temperate deciduous pollen taxa of *Corylus, Carpinus, and Quercus* reduced after 7 Ma. Therefore, the climate of this period is cooler compared with the climate earlier than 7 Ma. (Fig. 5). Moreover, the first axis of the PCA curve indicates greatly decreased values (most negative) also suggesting cooler climate (Fig. 10).

This enhanced cooling climate is in phase with the other records of the world, for instance, the IRD in the marine cores of the high latitude northern Hemisphere significantly increased at 7 Ma (e.g., Larsen et al., 1994; St. John and Krissek, 2002). This cooling climate may be also possibly CO_2 driven, evidenced by the abrupt and widespread increase in C4 biomass related to a decrease in atmospheric CO_2 concentrations (Cerling et al., 1997).

Since 5.23 Ma ago, the herb taxa especially *Artemisia* and Chenopodiaceae increased abruptly (Fig. 5). Modern pollen-rain data obtained from surface samples indicate that *Artemisia* prefers the cooler and more semi-arid environment of northern China (Sun et al., 1996). Therefore, the climate of this period indicates enhanced aridity in this region.

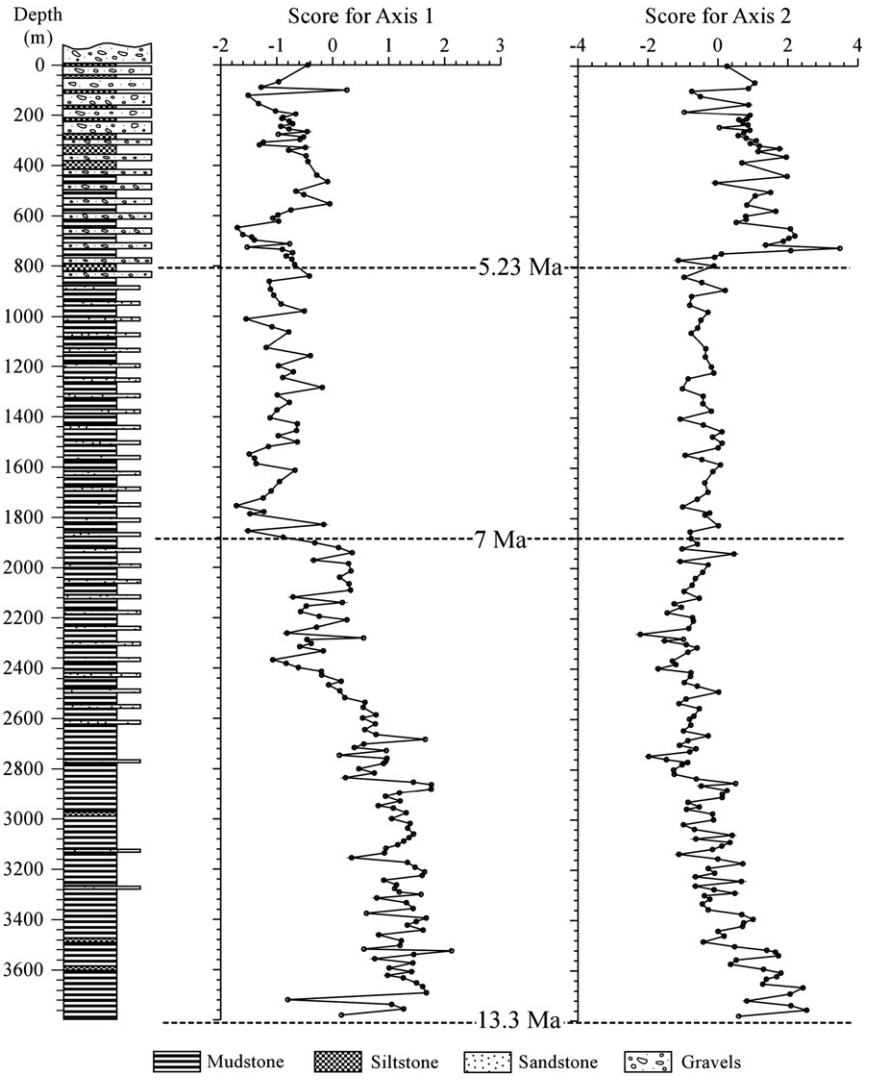

Fig. 10. Vertical variations in the factor scores of PCA axes 1 and 2 throughout the Kuchetawu section. Note the decrease of the axis 1 loadings at 7 Ma, and the abrupt increase of the axis 2 loadings since 5.23 Ma ago.

Furthermore, the PCA biplot of pollen percentages indicate that Chenopodiaceae and *Artemisia* have strong positive loadings on axis 2 (Fig. 8). Because both Chenopodiaceae and *Artemisia* grow in arid and semi-arid regions, the enhanced arid climate can be also demonstrated by the abrupt increasing values (towards more positive loadings) of PCA axis 2 after 5.23 Ma (Fig. 10).

The enhanced aridity after 5.23 Ma can be supported by several lines of evidence. Buried eolian siltstone in the southern marginal Tarim Basin indicates that the Taklamakan Desert occurred at least 5.3 Ma ago, marked extremely by arid climate prevailing in the Tarim Basin (Sun and Liu, 2006; Sun et al., 2008). Pollen data from Central Nepal also suggest climatic cooling at ~6.5–5 Ma, evidenced by an increase in the proportion of steppe taxa and a decrease in tropical forest taxa (Hoorn et al., 2000).

5.5. Comparison the pollen records from the foreland basins between the northern and southern Tianshan range

In a recent paper, we yielded a pollen diagram covering an age range of 26.6–2.6 Ma from the Taxihe section in the foreland basin of the northern Tianshan range (Fig. 11), which indicates mid-Miocene climatic optimum (18–15 Ma) and enhanced aridity after 6 Ma (Sun and Zhang, 2009). Compared with the pollen record of the Kuchetawu section in the foreland basin of the southern Tianshan range, both records document the enhanced arid event since the latest Miocene. Considering the uncertainty of the magnetostratigraphy, the enhanced aridity at 5.23 Ma in the southern Tianshan (the Tarim Basin) can be comparable to the strengthened drought climate at 6 Ma in the northern Tianshan (the Junggar Basin, Fig. 11).

The only difference between them is that the abrupt increase of high-altitude pollen *Abies* at 7 Ma in the southern Tianshan is not observed in the pollen spectra of the north. Such difference can be explained by the different topography and moisture sources of the two inland basins.

The Junggar Basin is bounded by the Tianshan range to the south, and the Altai Mountains to the northeast. But, in the northwest and the west of the basin, there are several mountain gaps allowing moist air masses from the Arctic and Atlantic Oceans to transport enough moisture to this basin (Fig. 11). In this sense, the climate and vegetation of the Junggar Basin is not very sensitive to the uplift of the northern Tianshan. However, the Tarim Basin is bounded by the Tianshan range to the north, the Pamir to the west, and the Kunlun range to the south (Fig. 11). The water vapor from the Indian Ocean hampered by the Himalaya can hardly reach the Tarim Basin. The Arctic water source can be blocked by the uplifted Tianshan range (Fig. 11). In this sense, the climate of the Tarim Basin is more sensitive

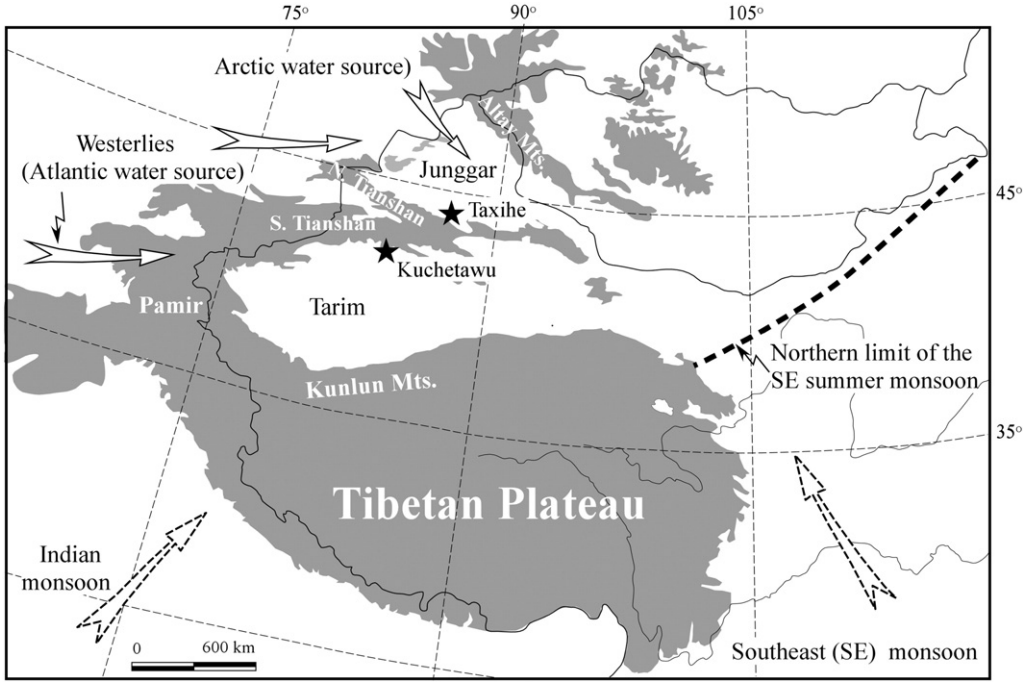

Fig. 11. Different water sources affecting the climate of the Tarim and Junggar basins. The dashed line indicates the northern limit of the southeast summer monsoon.

to the rainshadow effect of the Tianshan range. This can explained why there are some differences in the pollen record between the northern and southern Tianshan.

6. Conclusion

The studied Kuchetawu section in the northern foreland basin of the southern Tianshan range not only allows us to reconstruct the Neogene paleoenvironmental changes but also to disucss the interply between tectonic uplift and climatic change in an active tectonic region.

Generally, our pollen spectra were dominated by tree pollens between 13.3 and 2.6 Ma. The pollen taxa from ca. 13.3 to 7 Ma, preceded by a major regional uplift, were response to global climatic changes. A relatively warm and humid climate prevailed from 13.3 to 7 Ma. After 7 Ma, the regional uplift was a partial factor affecting pollen taxa especially for the increase of the high-aititude *Abies*. Enhanced aridity occurred since the latest Miocene, except the effect of global cooling on the environmetal change in the Tarim Basin, the mountain uplifts played an important role in controlling the drought climate in the Tarim Basin through blocking the Indian, Atlantic and Arctic water sources to the interior of the Tarim Basin.

Acknowledgements

This work was supported by the National Basic Research Program of China (2010CB833400), the Chinese Academy of Sciences (KZCX2-YW-Q09-06-04 and KZCX2-YW-130), and the National Nature Science Foundation of China (Grant 40830104). We thank Dr. Andreev and an anonymous reviewer for their critic comments on an earlier version of the manuscript.

References

Allen, M.B., Windley, B.F., Zhang, C., 1992. Palaeozoic collisional tectonics and magmatism of the Chinese Tien Shan, Central Asian. Tectonophysics 220, 89–115.
Avouac, J.P., Tapponnier, P., Bai, M., Hou, Y., Wang, G., 1993. Active thrusting and folding along the northeastern Tienshan, and rotation of Tarim relative to Dzungaria and Kazakhstan. Journal of Geophysical Research 98, 6755–6804.
Burchfiel, B.C., Brown, E.T., Deng, Q.D., Feng, X.Y., Li, J., Molnar, P., Shi, J.B., Wu, Z.M., You, H.C., 1999. Crustal shortening on the margins of the Tien Shan, Xinjiang, China. Intertional Geology Reviews 41, 665–700.
Cande, S.C., Kent, D.V., 1995. Revised calibration of the geomagnetic polarity timescale for the Late Cretaceous and Cenozoic. Journal of Geophysical Research 100, 6093–6095.
Cerling, T.E., Harris, J.M., MacFadden, B.J., Leakey, M.G., Quade, J., Eisenmann, V., Ehleringer, J.R., 1997. Global vegetation change through the Miocene/Pliocene boundary. Nature 389, 153–158.
Charreau, J., Gilder, S., Chen, Y., Dominguez, S., Avouac, J.P., Sen, S., Jolivet, M., Li, Y., Wang, W., 2006. Magnetostratigraphy of the Yaha section, Tarim Basin (China): 11 Ma acceleration in erosion and uplift of the Tian Shan mountains. Geology 34, 181–184. doi:10.1130/G22106.1.
Charreau, J., Chen, Y., Gilder, S., Barier, L., 2008. Comment on "Magnetostratigraphic study of the Kuche Depression, Tarim Basin, and Cenozoic uplift of the Tian Shan Range, Western China". Earth and Planetary Science Letters 268, 325–329.
Deng, T., 2006. Chinese Neogene mammal biochronology. Vertebrate PalAsiatic 44, 143–163.
Deng, T., Wang, X.M., 2004. Late Miocene *Hipparion* (Equidae, Mammalia) of eastern Qaidam Basin in Qinghai, China. VertPalAsiat 42, 316–333.
Deng, Q.D., Feng, X.Y., Zhang, P.Z., Xu, X.W., Yang, X.P., Peng, S.Z., Li, J., 2000. Active Tectonics of the Tianshan Mountains. Seismology Press, Beijing, p. 399.
Faegri, K., Iversen, J., 1989. Textbook of Pollen Analysis. John Wiley & Sons, New York, p. 328.
Fu, B.H., Lin, A.M., Kano, K., Maruyama, T., Guo, J.M., 2003. Quaternary folding of the eastern Tianshan, Northwest China. Tectonophysics 369, 79–101.
Fu, B.H., Ninomiya, Y., Guo, J.M., 2010. Slip partitioning in the northeast Pamir–Tian Shan convergence zone. Tectonophysics 483, 344–364.
Gao, J., Li, M.S., Xiao, X.C., Tang, Y.Q., He, G.Q., 1998. Paleozoic tectonic evolution of the Tianshan Orogen, northwestern China. Tectonophysics 287, 213–231.
Hendrix, M.S., Dumitru, T.A., Graham, S.A., 1994. Late Oligocene–early Miocene unroofing in the Chinese Tian Shan: an early effect of the India–Asia collision. Geology 22, 487–490.
Hoorn, C., Ohja, T., Quade, J., 2000. Palynological evidence for vegetation development and climatic change in the Sub-Himalayan Zone (Neogene, Central Nepal). Palaeogeography, Palaeoclimatology, Palaeoecology 163, 133–161.
Hu, Z.H., Sarjeant, W.A.S., 1992. Cenozoic spore-pollen assemblage zones from the shelf of the East China Sea. Review of Palaeobotany and Palynology 72, 103–118.
Huang, T.K., Young, C.C., Cheng, Y.C., Chow, T.C., Bien, M.N., Weng, W.P., 1947. Report on geological investigation of some oil-fields in Sinkiang (Geology Memoirs, Series A, No. 21). The National Geology Survey China, Nanking, p. 118.
Huang, B.C., Piper, J.D.A., Peng, S.T., Liu, T., Li, Z., Wang, Q.C., Zhu, R.X., 2006. Magnetostratigraphic study of the Kuche Depression, Tarim Basin, and Cenozoic uplift of the Tian Shan Range, Western China. Earth and Planetary Science Letters 251, 346–364.
Huang, B.C., Piper, J.D.A., Zhu, R.X., 2008. Reply to the comment by J. Charreau et al. on "Magnetostratigraphic study of the Kuche Depression, Tarim Basin, and Cenozoic uplift of the Tian Shan Range, Western China". Earth and Planetary Science Letters 275, 404–406.

Hubert-Ferrari, A., Suppe, J., Gonzalez-Mieres, R., Wang, X., 2007. Mechanisms of active folding of the landscape (southern Tian Shan, China). Journal of Geophysical Research 112, B03S09. doi:10.1029/2006JB004362.

Jin, Z.J., Yang, M.H., Lu, X.X., Sun, D.S., Tang, X., Peng, G.X., Lei, G.L., 2008. The tectonics and petroleum system of the Qiulitagh fold and thrust belt, northern Tarim basin, NW China. Marine and Petroleum Geology 25, 767–777.

Larsen, H.C., Saunders, A.D., Clift, P.D., Beget, J., Wei, W., Spezzaferri, S., 1994. ODP Leg 152 Scientific Party, 1994. Seven million years of glaciation in Greenland. Science 13, 952–955.

Li, C.K., Wu, W.Y., Qiu, Z.D., 1984. Chinese Neogene: subdivision and correlation. VertPalAsiat 22, 163–178.

Liang, M.M., Bruch, A., Collinson, M., Mosbrugger, V., Li, C.S., Sun, Q.G., Hilton, J., 2003. Testing the climatic estimates from different palaeobotanical methods: an example from the Middle Miocene Shanwang flora of China. Palaeogeography, Palaeoclimatology, Palaeoecology 198, 279–301.

Liu, G.W., Leopold, E.B., 1994. Climatic comparison of Miocene pollen floras from northern East-China and south-central Alaska. Paleogeography, Paleoclimatology and Paleobotany 108, 217–228.

Ma, Y., Li, J., Fan, X., 1998. Pollen-based vegetational and climatic records during 30.6 to 5.0 Myr from Linxia area, Gansu. Chinese Science Bulletins 43, 301–304 (in Chinese).

Ma, Y., Fang, X., Li, J., Wu, F., Zhang, J., 2004. Vegetational and environmental changes during late Tertiary–early Quaternary in Jiuxi Basin. Science in China (Series D) 34, 107–116 (in Chinese).

Peng, X.L., 1975. Positions and stratigraphic control of the Cenozoic mammalian fossils in the Junggar Basin of Xinjiang. Vertebrata PalAsiatica 13, 185–189.

Shaw, P.J.A., 2003. Multivariate Statistics for the Environmental Sciences. Hodder Arnold, London, p. 233.

Sobel, E.R., Chen, J., Heermance, R.V., 2006. Late Oligocene–Early Miocene initiation of shortening in the Southwestern Chinese Tian Shan: implications for Neogene shortening rate variations. Earth and Planetary Science Letters 247, 70–81.

St. John, K.E.K., Krissek, L.A., 2002. The late Miocene to Pleistocene ice-rafting history of southeast Greenland. Boreas 31, 28–35.

Sun, J.M., Liu, T.S., 2006. The age of the Taklimakan Desert. Science 312, 1621.

Sun, X.J., Wang, P.X., 2005. How old is the Asia monsoon system? Palaeobotanical records from China. Palaeogeography, Palaeoclimatology, Palaeoecology 222, 181–222.

Sun, J.M., Zhang, Z.Q., 2008. Palynological evidence for the mid-Miocene climatic optimum recorded in Cenozoic sediments of the Tianshan Range, northwestern China. Global and Planetary Change 64, 53–68.

Sun, J.M., Zhang, Z.Q., 2009. Syntectonic growth strata and implications for late Cenozoic tectonic uplift in the northern Tian Shan, China. Tectonophysics 463, 60–68.

Sun, X.J., Song, C., Wang, F., 1996. Pollen-climate response surface of selected taxa from northern China. Science in China (Series D) 39, 486–493.

Sun, J.M., Zhu, R.X., Bowler, J., 2004. Timing of the Tianshan Mountains uplift constrained by magnetostratigraphic analysis of molasse deposits. Earth and Planetary Science Letters 219, 239–253.

Sun, J.M., Xu, Q.H., Huang, B.C., 2007. Late Cenozoic magnetochronology and paleoenvironmental changes in the northern foreland basin of the Tian Shan Mountains. Journal of Geophysical Research 112. doi:10.1029/2006JB004653.

Sun, J.M., Zhang, L.Y., Deng, C.L., Zhu, R.X., 2008. Evidence for enhanced aridity in the Tarim Basin of China since 5.3 Ma. Quaternary Science Reviews 27, 1012–1023.

Sun, J.M., Li, Y., Zhang, Z.Q., Fu, B.H., 2009. Magnetostratigraphic data on the Neogene growth folding in the foreland basin of the southern Tianshan Mountains. Geology 37, 1051–1054.

Tang, L.J., Jia, C.Z., Jin, Z.J., Chen, S.P., Pi, X.J., Xie, H.W., 2004. Salt tectonic evolution and hydrocarbon accumulation of Kuqa foreland fold belt, Tarim Basin, NW China. Journal of Petroleum Science and Engineering 41, 97–108.

ter Braak, C.J.F., Smilauer, P., 2002. CANOCO Reference Manual and CanoDraw for Windows User's Guide: Software for Canonical Community Ordination (version 4.5). Microcomputer Power, Ithaca, NY, p. 500.

Wang, W.M., 1990. Sporo-pollen assemblages from the Miocene Tonggure formation of Inner Mongolia and its climate. Acta Botanica Sinica 32, 901–904.

Wang, F.X., Qian, N.F., Zhang, Y.L., Yang, H.Q., 1997. Pollen Flora of China. Science Press, Beijing, p. 461.

Xu, J.X., Ferguson, D.K., Li, C.S., Wang, Y.F., 2008. Late Miocene vegetation and climate of the Lühe region in Yunnan, southwestern China. Review of Palaeobotany and Palynology 148, 36–59.

Yin, A., Nie, S., Craig, P., Harrison, T.M., Ryerson, F.J., Qian, X., Yang, G., 1998. Late Cenozoic Tectonic evolution of the southern Chinese Tian Shan. Tectonics 17, 1–27.